Journal of Alloys and Compounds 509 (2011) 5029–5032

Contents lists available at ScienceDirect

Journal of Alloys and Compounds

journal homepage: www.elsevier.com/locate/jallcom

Investigation on the low-frequency mechanical properties of $La_{0.6}Sr_{0.4}Co_{1-x}Fe_xO_{3-\delta}$ materials

Wu Xiu Sheng[a], Cao Ju Fang[a], Kong Hui[c], Chen Zhi Jun[b], Liu Wei[b,*]

[a] Anhui Key Laboratory of Advanced Building Material, Department of Materials Science and Engineering, Anhui Institute of Architecture & Industry, Hefei, Anhui 230026, PR China
[b] Laboratory of Advanced Functional Materials and Devices, Department of Materials Science and Engineering, University of Science and Technology of China, Hefei, Anhui 230022, PR China
[c] School of Metallurgy and Resources, Anhui University of Technology, Maanshan, Anhui 243002, PR China

ARTICLE INFO

Article history:
Received 6 October 2010
Received in revised form
19 November 2010
Accepted 22 November 2010
Available online 30 November 2010

PACS:
62.40.+I
61.72.Hh
75.60.−d

Keywords:
Ceramics
Mechanical properties
Phase transitions
Domain structure

ABSTRACT

The low-frequency mechanical properties of $La_{0.6}Sr_{0.4}Co_{1-x}Fe_xO_{3-\delta}$ ($0 \le x \le 0.8$) materials have been measured using a computer-controlled pendulum. For undoped sample, five internal friction peaks (P0, P1, P2, P3 and P4) were observed. However, with the Fe doping, only two peaks (P3 and P4) were found at high temperature. The peaks of P0 and P1 have the feature of phase transition-induced internal friction, while the peaks of P2, P3 and P4 are the relaxation-type. From the analysis, it is suggested that the peak of P0 is due to the phase separation and the peak of P1 is related to the ferromagnetic (FM)–paramagnetic (PM) phase transition. For the peaks of P2, P3 and P4, they were associated with the motion of domain walls. The formation of this kind of domain structure is a consequence of a transformation from the paraelastic cubic phase to ferroelastic rhombohedral phase.

1. Introduction

$LaCoO_3$-based materials have attracted considerable attention because of their fascinating physical phenomenon such as spin-state transition [1], and magnetic phase separation [2–8], as well as their potential materials as oxygen permeable membranes [9]. The parent compound $LaCoO_3$ has a rhombohedrally distorted pseudo-cubic structure with the space group $\boldsymbol{R\bar{3}c}$. This distortion decreases monotonically with the strontium doping in $La_{1-x}Sr_xCoO_3$, and the structure becomes cubic when $x = 0.6$ [10]. The magnetic properties of this system are also strongly dependent on the strontium content. At low doping level, the $La_{1-x}Sr_xCoO_3$ system runs into a spin-glass phase, when $x \ge 0.2$, this system becomes ferromagnetically ordered [2–4]. However, some evidences suggest that even below the ferromagnetic ordering temperature T_C, the system is still a cluster-glass phase with short range ferromagnetic ordering [5–7].

Recently, the attention of researchers was concentrated on the ferroelasticity of the $LaCoO_3$-based system [11–18]. But till now, its origin is still in discussion. By means of in situ transmission electron microscopy (TEM) during thermal cycles, different types of structural features of $LaCoO_3$-based materials, such as twins and antiphase domains have been observed by Orlovskaya et al. The domain motion and de-twinning during heating, and the reappearance of twins during cooling may be responsible for ferroelastic behavior [14]. Vullum et al. also confirmed this conclusion by the measurement of in situ synchrotron X-ray diffraction [15]. However, although similar ferroelastic behavior has been found in $La_{0.6}Sr_{0.4}FeO_3$, Orlovskaya et al. suggested that this behavior originates from the phase transformation and/or dislocation motion since no domain/twin structure was observed [19].

As a systematic tool, the internal friction technique has been proven to be particularly successful in investigating the microscopic relaxation processes and phase transitions in solid materials [20–25]. To gain more insight into the microscopic origin of the inelasticity and phase transition in $LaCoO_3$-based materials, the low-frequency mechanical properties of $La_{0.6}Sr_{0.4}Co_{1-x}Fe_xO_{3-\delta}$ ($0 \le x \le 0.8$) are investigated in this paper. Furthermore, the measurements of resistivity and magnetization are also carried out to clarify the nature of the internal friction peaks.

* Corresponding author.
E-mail addresses: wxs@aiai.edu.cn (X.S. Wu), wliu@ustc.edu.cn (W. Liu).

0925-8388/$ – see front matter © 2010 Elsevier B.V. All rights reserved.
doi:10.1016/j.jallcom.2010.11.127

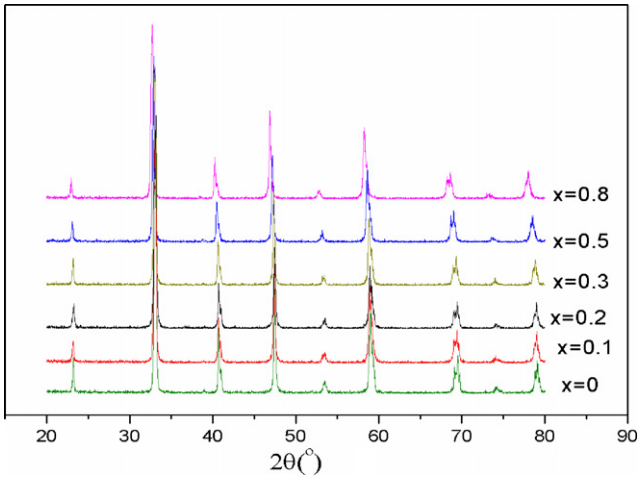

Fig. 1. XRD patterns of $La_{0.6}Sr_{0.4}Co_{1-x}Fe_xO_{3-\delta}$ at room temperature.

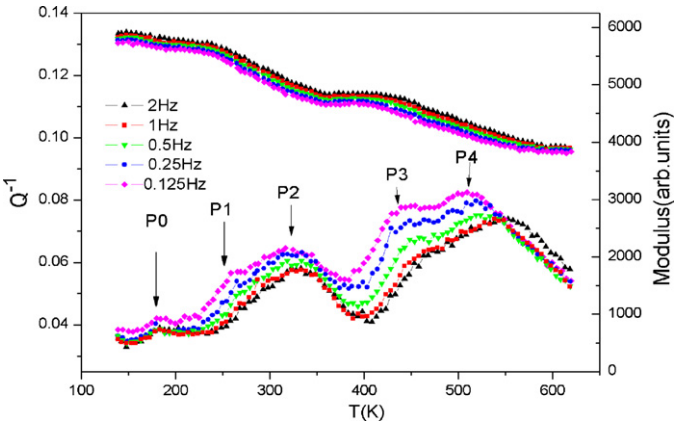

Fig. 2. Temperature dependence of the shear modulus and internal friction of $La_{0.6}Sr_{0.4}CoO_{3-\delta}$ with various frequencies.

2. Experimental procedure

$La_{0.6}Sr_{0.4}Co_{1-x}Fe_xO_{3-\delta}$ ($0 \le x \le 0.8$) powders were prepared via a citrate route. Two aqueous solutions of iron nitrate and cobalt nitrate were firstly prepared and analyzed by titrations to determine the concentration of Fe and Co ions. Then these solutions were mixed together with the appropriate amounts of La_2O_3 (99.9%) and $SrCO_3$ (>99.0%), which were both completely dissolved by adding diluted nitric acid. After forming a clear solution, citric acid was added at a molar ratio of citric acid: metal ions = 1.5:1.0, followed by adjusting the pH value to 2–3. The solution was subsequently stirred and evaporated at 80 °C until a formation of polymeric precursor, which was ignited in air to remove the organic contents. The resulting ash was ground to fine powders and calcined at 1050 °C in air for 5 h. The obtained powders were uniaxially pressed into bars at 150 MPa, subsequently isostatically pressed at 300 MPa and sintered in air at 1250 °C for 10 h. Since the crystal structure of $La_{1-y}Sr_yCo_{1-x}Fe_xO_{3-\delta}$ is dependent on cooling rate [26], in order to obtain purely rhombohedral phase sample, the cooling rate of 1 K/min is adopted.

The crystal structure of the calcined powders was characterized by XRD (Philips X'Pert Pro Super, Cu Kα). The electrical resistivity was measured by standard four-probe technique. The zero-field-cooled (ZFC) magnetization was measured in an external magnetic field of 100 Oe using a commercial quantum device (superconducting quantum interference device; Quantum Design MPMSXL). The internal friction and shear modulus were measured in a computer-controlled automatic inverted torsion pendulum using the forced-vibration method with the maximum torsion strain amplitude kept at 1.5×10^{-5} at a heating rate of 2 K/min from 120 K to 650 K.

3. Experimental results and discussion

The X-ray diffraction patterns of $La_{0.6}Sr_{0.4}Co_{1-x}Fe_xO_{3-\delta}$ ($x = 0$, 0.1, 0.2, 0.3, 0.5, 0.8) are shown in Fig. 1. All the samples crystallize in single phase and exhibit a rhombohedrally distorted perovskite structure with $\boldsymbol{R\bar{3}c}$ symmetry, which is in accordance with the earlier studies [6].

Fig. 2 presents the temperature dependence of internal friction Q^{-1} and shear modulus M for $La_{0.6}Sr_{0.4}CoO_{3-\delta}$. Four internal friction peaks are readily observed and marked as P0, P2, P3 and P4, which locate at about 180, 320, 440, and 505 K. Besides these peaks, another small shoulder peak is also found which locates at the low temperature side of P2 and is marked as P1 (255 K). For P0 and P1, their positions do not shift with increasing the frequency, which reveals that the two peaks are both phase transition-induced internal friction peaks. However, the peaks of P2, P3 and P4 are of relaxation type, since their peak temperature shifts to higher temperature with increasing the frequency. For the peaks of P0 and P1, from the earlier reports, no structure phase transitions have been observed in this temperature range. So there should be other reasons for these two peaks.

In order to clarify the origin of the peaks of P0 and P1, the measurements of the magnetic and electric transport properties were carried out. The results are shown in Fig. 3. It can be seen that the ZFC magnetization rises sharply at around 250 K, corresponding to a PM–FM phase transition, and then undergoes a less rapid drop down to 40 K. However, the resistivity shows a monotonic descending, and only a slope change is seen at the Curie temperature T_c, which is regarded as a result of spin–disorder scattering. These results agree well with the earlier reports [6]. Combined with the results of magnetization and resistivity as shown in Fig. 3, the peak of P1 at 255 K is suggested to be related with the magnetic transition, while the origin of the peak of P0 is still unclear. Therefore, we considered other alternative mechanisms which could cause this internal friction peak.

According to the phase diagram of $La_{1-x}Sr_xCoO_3$ [3,8], it is postulated that in the low doping region ($x < x_m$, $x_m \sim 0.2$), the sample separates into hole-rich ferromagnetic clusters and hole-poor nonferromagnetic matrix. The former is dominated by the ferromagnetic double exchange interaction between Co^{3+} and Co^{4+}, and the latter is dominated by the antiferromagnetic (AF) superexchange interaction between Co^{3+} and Co^{3+}. Furthermore, the ferromagnetic clusters are embedded in the nonferromagnetic matrix, and the competition between the ferromagnetic and the antiferromagnetic interactions along with the randomness lead to spin glass (SG) states. With increasing the x, the ferromagnetic double-exchange interaction is enhanced, and these ferromagnetic clusters eventually coalesce, leading to the appearance of the cluster glass phase with short range ferromagnetic ordering ($x_m < x < 0.50$). According to this phase diagram, our sample $La_{0.6}Sr_{0.4}CoO_{3-\delta}$ should belong to the cluster glass phase. In fact, this coexistence of two phases has been experimental confirmed

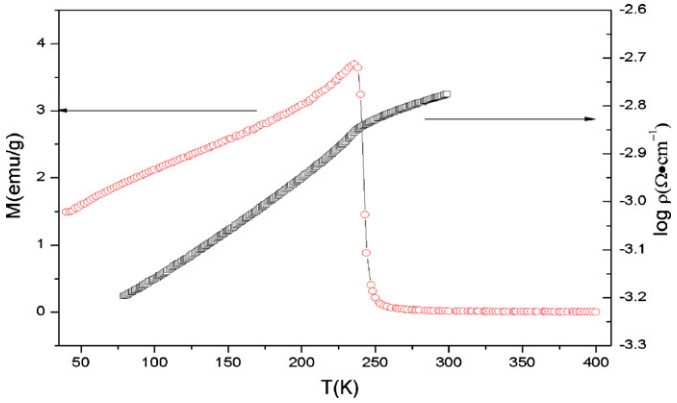

Fig. 3. The variation of the magnetization [$M(T)$] in a field of 100 Oe (zero-field-cooled and taken on heating) and the logarithmic of the resistivity (on heating) with temperature for $La_{0.6}Sr_{0.4}CoO_{3-\delta}$.

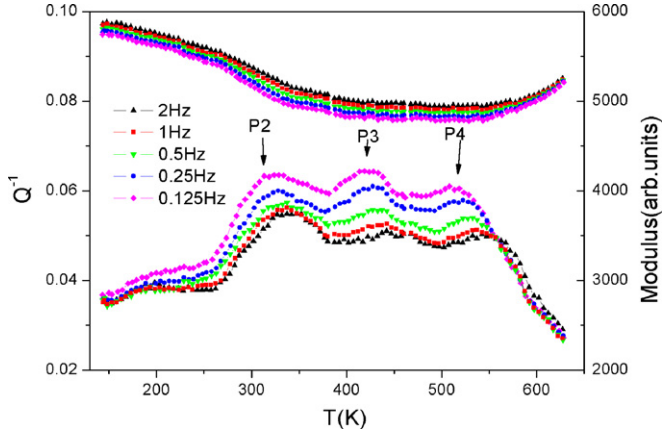

Fig. 4. Temperature dependence of the shear modulus and internal friction of $La_{0.6}Sr_{0.4}Co_{0.9}Fe_{0.1}O_{3-\delta}$ with various frequencies.

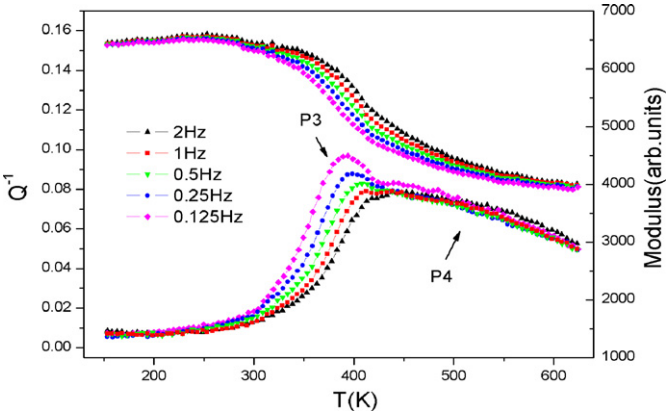

Fig. 6. Temperature dependence of the shear modulus and internal friction of $La_{0.6}Sr_{0.4}Co_{0.7}Fe_{0.3}O_{3-\delta}$ with various frequencies.

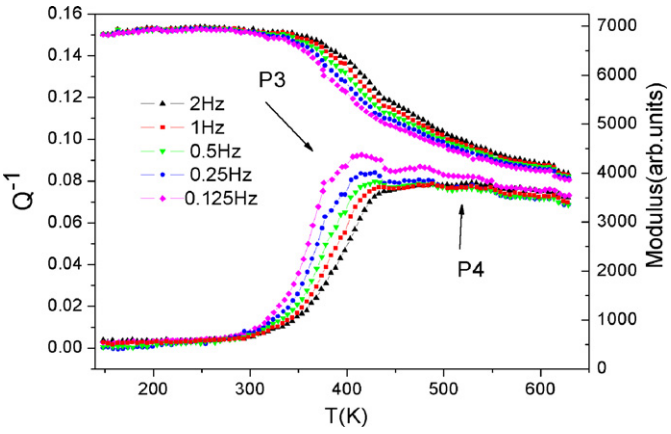

Fig. 7. Temperature dependence of the shear modulus and internal friction of $La_{0.6}Sr_{0.4}Co_{0.5}Fe_{0.5}O_{3-\delta}$ with various frequencies.

by Kuhns et al. [8]. In manganites, it is known that this kind of phase coexistence always leads the internal friction peak [24,25]. Thus, it is highly possible that the peak of P0 may originate from the phase separation.

With the substitution of Fe ions for Co ions in $La_{0.6}Sr_{0.4}Co_{1-x}Fe_xO_3$, some different low frequency mechanical behaviors are observed. Figs. 4 and 5 show the results of the samples ($x = 0.1$, 0.2), respectively. It can be seen that the peaks of P2, P3 and P4 still exist at the corresponding temperature range. But the peaks of P0 and P1 cannot be readily found. With increasing the Fe content, the peak of P2 is disappeared. The curves of $Q^{-1}(T)$ and $M(T)$ for the samples ($x = 0.3$, 0.5 and 0.8) are, respectively, shown in Figs. 6–8. Three compositions exhibit the similar low-frequency mechanical behaviors. Only one peak is readily observed, and at high temperature side of this peak, an obvious abnormity is found, which suggests the existence of another peak. Compared with the curves in Figs. 2–5, the former corresponds to the peak of P3, and the latter is related to the peak of P4.

Compared with the peaks of P0 and P1, the other three peaks (P2, P3 and P4) are much broader in the curves of $Q^{-1}(T)$, implying they have a fully different origin. As we known, it has been reported that $LaCoO_3$-based perovskites exhibit a nonlinear stress–strain relationship and inelastic deformation behavior [11–17]. For our investigated $La_{0.6}Sr_{0.4}Co_{1-x}Fe_xO_3$ system, at high temperature, the lattice structure of $La_{0.6}Sr_{0.4}Co_{1-x}Fe_xO_3$ system is cubic symmetry. When decreasing temperature to a critical point (for $La_{0.6}Sr_{0.4}CoO_3$, about 673 K [29]), the system undergoes a transition from cubic to rhombohedral symmetry, driven by rotation of the $Co(Fe)O_6$-octahedra about one of the cubic three-fold symmetry axis. Due to the choice of four equivalent triad axes, transformation twin domains can be formed, which have been confirmed by the transmission electron microscopy [14]. The combination of structure changes and the appearance of transformation twins result in a rapid softening in modulus even in small applied forces. Low-frequency internal friction measurement on $La_{1-x}Sr_xFeO_3$ has

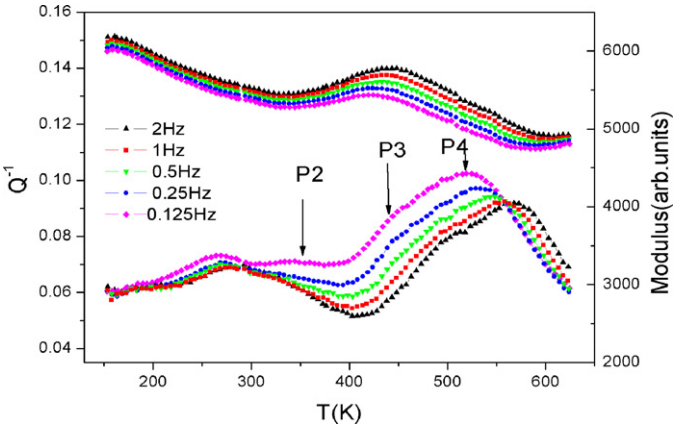

Fig. 5. Temperature dependence of the shear modulus and internal friction of $La_{0.6}Sr_{0.4}Co_{0.8}Fe_{0.2}O_{3-\delta}$ with various frequencies.

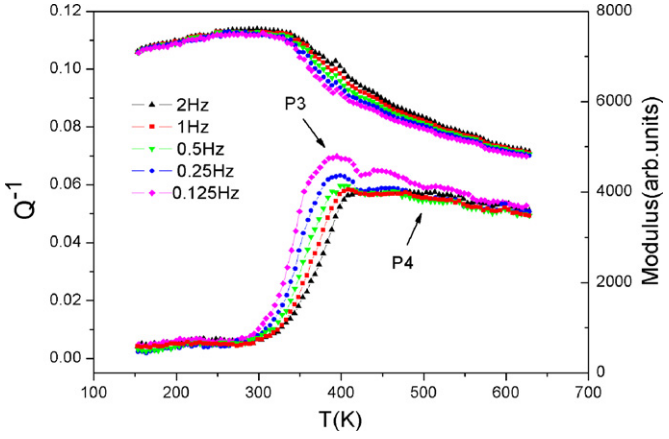

Fig. 8. Temperature dependence of the shear modulus and internal friction of $La_{0.6}Sr_{0.4}Co_{0.2}Fe_{0.8}O_{3-\delta}$ with various frequencies.

demonstrated this point [20,21]. The inelastic deformation of $LaCo(Fe)O_3$ based perovskites may associated with the structure phase transition and the appearance of transformation twins.

In many ferroelectric ceramics, the motion of the domain walls leads to the relaxation internal friction peaks [27,28]. Thus, the similar feature may be response to the three peaks (P2–P4) in our samples. The domain forms during phase transition, and when the temperature is high enough, thermal energy is sufficient to allow these domain walls to move under small applied forces. This is accompanied by an increase in Q^{-1} (P4 peak), as energy is dissipated by moving domain walls against the force exerted by lattice defects. Moreover, Peierls force associated with moving a wall of finite thickness through a discrete lattice may also contribute small part to this peak [27]. With the temperature decreasing, thermal energy is so low that it is not enough to overcome the interactions between oxygen vacancies and domain walls. Thus these domain walls become immobile. This freezing of the domain walls is anelastic and would lead to the pronounced resonance peak [20,21]. This phenomenon is very similar to those of $LaAlO_3$ [30] and $Ca_{1-x}Sr_xTiO_3$ [31] reported by Harrison. In fact, in the $LaCoO_3$-based perovskites, different types of domains have been confirmed by the in situ TEM measurement, such as short parallel domains oriented at 180° to each other and long domains [14]. Upon heating, the 180° domains are found to be the most unstable and mobile, but other long domains are still stable. Therefore, it is suggested that the peaks of P2 and P3 may originate from the movement of the different domain walls.

Since the ionic radius of Fe ions is larger than that of Co ions, its substitution involves a tilting of the octahedron and increases the distortion of the perovskite cell. It is known that the formation of the transformation twins and domain originates from the choice of four equivalent triad axes that the octahedral rotation could occur. Thus the tilting of the octahedron may have significant effect on the formation of domain state, leading to the different microstructure. In fact, in the $La_{0.6}Sr_{0.4}FeO_3$, no domains, twins, antiphase boundaries, stacking faults, and other planar defects are observed [19], which is different to the $LaCoO_3$ based perovskites. Thus in the higher Fe-doping samples, different mechanical response is observed, and it can be seen that the peak of P2 disappears. However, it should be mentioned that the effect of Fe doping on the formation of the transformation twins and domain is still under discussion. Different conclusions have been drawn through different experimental conditions. For example, recently, the micro-structural evidence of domains in the rhombohedral $La_{0.58}Sr_{0.4}Co_{0.2}Fe_{0.8}O_{3-\delta}$ sample is confirmed by the SEM and TEM observations [26]. Thus, more detailed studies are needed to further clarify the nature of the domain walls.

4. Conclusion

At most five internal friction peaks are observed depending on Fe content in the $La_{0.6}Sr0_{.4}Co_{1-x}Fe_xO_{3-\delta}$ perovskites: three are relaxation peaks and two are phase transition type peaks. In addition to the peak of P1 correlated with PM–FM transition, the peak of P0 located below T_c is suggested to originate from the phase separation. At higher temperature, the system undergoes a transition from cubic to rhombohedral phase on cooling, accompanied by the formation of transformation twins. These relaxation peaks should be related to the motion of domain walls. The ferroelastic behavior of the Fe-doped $La_{0.6}Sr_{0.4}CoO_3$ may associate with the structure transition and the motion of the domain walls.

Acknowledgments

The research was supported by National Natural Science Foundation of China (Grant Nos. 10574123 and 11004002), the Key Program of Scientific Research Fund of Anhui Provincial Education Department (No. KJ2008A018) and the doctoral initial funding of Anhui University of Architecture (2008).

References

[1] C. Zobel, M. Kriener, D. Bruns, J. Baier, M. Gruninger, T. Lorenz, P. Reutler, A. Revcolevschi, Phys. Rev. B 66 (2002), 020402(R)-1–4.
[2] M. Itoh, I. Natori, S. Kubota, K. Motoya, J. Phys. Soc. Jpn. 63 (1994) 1486–1493.
[3] M.A. Senaris-Rodriguez, J.B. Goodenough, J. Solid State Chem. 118 (1995) 323–336.
[4] M.J.R. Hoch, P.L. Kuhns, W.G. Moulton, A.P. Reyes, J. Wu, C. Leighton, Phys. Rev. B 69 (2004) 014425-1–014425-7.
[5] S. Mukherjee, R. Ranganathan, P.S. Anilkumar, P.A. Joy, Phys. Rev. B 54 (1996) 9262–9274.
[6] J. Wu, C. Leighton, Phys. Rev. B 67 (1999) 174408-1–174408-16.
[7] R. Caciuffo, D. Rinaldi, G. Barucca, J. Mira, J. Rivas, M.A. Señarís-Rodríguez, P.G. Radaelli, D. Fiorani, J.B. Goodenough, Phys. Rev. B 59 (1999) 1068–1078.
[8] P.L. Kuhns, M.J.R. Hoch, W.G. Moulton, A.P. Reyes, J. Wu, C. Leighton, Phys. Rev. Lett. 91 (2003) 127202-1–127202-4.
[9] H.J.M. Bouwmeester, Solid State Ionics 82 (2003) 141–150.
[10] A.N. Petrov, O.F. Kononchuk, A.V. Andreev, V.A. Cherepanov, P. Kofstad, Solid State Ionics 80 (1995) 189–199.
[11] N Orlovskaya, K. Kleveland, T. Grande, M.-A. Einarsrud, J. Eur. Ceram. Soc. 20 (2000) 51–56.
[12] K. Kleveland, N. Orlovskaya, T. Grande, A.M.M. Moe, M.A. Einarsrud, K. Breder, G. Gogotsi, J. Am. Ceram. Soc. 84 (2001) 2029–2033.
[13] N. Orlovskaya, Y. Gogotsi, M. Reece, B. Cheng, I. Gibson, Acta Mater. 50 (2002) 715–723.
[14] N. Orlovskaya, N. Browning, A. Nicholls, Acta Mater. 51 (2003) 5063–5071.
[15] P.E. Vullum, J. Mastin, J. Wright, M.A. Einarsrud, R. Holmestad, T. Grande, Acta Mater. 54 (2006) 2615–2624.
[16] N. Orlovskaya, D. Steinmetz, S. Yarmolenko, D. Pai, J. Sankar, J. Goodenough, Phys. Rev. B 72 (2005) 014122-1–014122-7.
[17] S. Faaland, T. Grande, P.E. Vullum, R. Holmestad, M.-A. Einarsrud, J. Am. Ceram. Soc. 88 (2005) 726–730.
[18] N. Orlovskaya, M. Lugovy, S. Pathak, D. Steinmetz, J. Lloyd, L. Fegely, M. Radovic, E.A. Payzant, E.L. Curzio, L.F. Allard, J. Kuebler, J. Power Sources 182 (2008) 230–239.
[19] N. Orlovskaya, H. Anderson, M. Brodnikovskyy, M. Lugovy, M.J. Reece, J. Appl. Phys. 100 (2006) 026102-1–026102-3.
[20] X.S. Wu, Y.B. Zuo, J.H. Li, C.S. Chen, W. Liu, J. Alloys Compd. 462 (2008) 432–435.
[21] X.S. Wu, C.L. Yang, Z.J. Chen, C.S. Chen, W. Liu, Acta Phys. Sin. 9 (2009) 6419–6425 (in Chinese).
[22] W.L. Warren, K. Vanheusden, D. Dimos, G.E. Pike, B.A. Tuttle, J. Am. Ceram. Soc. 79 (1996) 536–538.
[23] X.P. Wang, Q.F. Fang, Phys. Rev. B 65 (2002) 064304-1–064304-6.
[24] Y.Q. Ma, W.H. Song, R.L. Zhang, J.M. Dai, J. Yang, J.J. Du, Y.P. Sun, C.Z. Bi, Y.J. Ge, X.G. Qiu, Phys. Rev. B 69 (2004) 134404-1–134404-6.
[25] W.J. Lu, Y.P. Sun, B.C. Zhao, X.B. Zhu, W.H. Song, Phys. Rev. B 73 (2006) 214409-1–214409-6.
[26] B.X. Huang, J. Malzbender, R.W. Steinbrech, E. Wessel, H.J. Penkalla, L. Singheiser, J. Membr. Sci. 349 (2010) 183–188.
[27] Y.N. Wang, Y.N. Huang, H.M. Shen, Z.F. Zhang, J. Phys. IV 6 (Colloque C8, Suppl. to J. Phys. III) (1996) 505–514.
[28] J.A. Bartkowska, J. Bluszcz, R. Zachariasz, J. Milczuk, B. Brus, J. Phys. IV Fr. 137 (2006) 19–21.
[29] S.R. Wang, M. Katsuki, M. Dokiya, T. Hashimoto, Solid State Ionics 159 (2003) 71–78.
[30] R.J. Harrison, S.A.T. Redfern, Phys. Earth Planet. Int. 134 (2002) 253–272.
[31] R.J. Harrison, S.A.T. Redfern, J. Street, Am. Mineral. 88 (2003) 574–582.